

The influence of the oxygen donor capacity of polystearylmethacrylate over polyethylene bulk density when using modified methylaluminoxane as co-catalyst

Odilia Pérez-Camacho and Eduardo Cardozo-Villalba*

Departamento de Química Macromolecular y Nanomateriales, Centro de Investigación en Química Aplicada, 25294, Saltillo, Coahuila, México

Received: 12 January 2022, Accepted: 16 February 2022

ABSTRACT

In this work, the interaction between a polystearylmethacrylate ($M_n = 8,900 \text{ g mol}^{-1}$, $X_n = 26$, $D = 1.1$) and modified methylaluminoxane 12 (MMAO-12) co-catalyst is studied using different spectroscopic methods. The effect of this oxygen-donor additive was measured by the changes in the bulk density of the raw polyethylene, which resulted increased respect to those obtained in blank reactions. A decrease in the activity was also observed as a penalty for the improvement of the bulk density, enhancing the possibility of reducing fouling. The coordination of the carbonyl oxygen groups of polystearylmethacrylate to aluminum (III) centers is confirmed by $^1\text{H-NMR}$ and FTIR studies, and by a simple semi-empirical computational calculation. A method for obtaining a tri-component co-catalyst mixture is described using the methyl-bridging capacity of trimethylaluminum and its Lewis acidity to get the polystearylmethacrylate and MMAO-12 linked together. This robust adduct introduces a hierarchy over the PE chain growing, leading to higher bulk densities for PE beads (0.43 g cm^{-3}) concerning blank reactions (0.26 g cm^{-3}). *Polyolefins J* (2022) 9: 93-101

Keywords: Metallocene catalyst; oxygen donors; methylaluminoxane; ethylene polymerization; bulk density.

INTRODUCTION

Polyolefins (PO's) are ranked as high-demand polymers compared to others with similar characteristics, e.g., polystyrene (PS), polyvinyl chloride (PVC), and polyesters. Roughly, 10% of the polyolefins produced worldwide are synthesized by employing metallocenes. Depending on their mechanical-physical properties, they are classified as specialty or engineering polymers with a

lower cost than polymers from step-growing or ring-opening polymerization (ROP) processes.

Sinn and Kaminsky have made several contributions to traditional coordination catalysis for olefin polymerization based on metallocene/methylaluminoxane (MAO) systems [1-3]. Today, the volume of polyethylene production by this route, as well as the good perfor-

* Corresponding Author - E-mail: cardozoej.d17@ciqa.edu.mx

mance in typical reactions, has made polyethylene synthesis an active research niche. Furthermore, there has been a fast growth in new materials that serve as co-catalyst and/or catalyst support as specially noted in the research of Lee [4,5] and Pothirat [6] to improve and find new applications to polyethylenes or just to make the process even more profitable.

The coordination chemistry of aluminum (III) can be advantageous in the formation of active species due to the high polarization given by ligands with oxygen atoms as donors [7], producing more labile H₃C-Al bonds, which is considered the most important phenomena in the activation process when using metallocenes, as described by McIndoe [8 - 10] and Linolatti [11].

Likewise, the use of computational chemistry to the better understanding of complex systems has become mandatory currently [12 - 14]. Semi-empirical methods have proved to be the best choice to model and calculate polymers, proteins, or molecules structures with more than 100 atoms due to their accuracy and low computational cost [15, 16], allowing to obtain quick and representative results for a molecular system. As evidenced in this work, to interpret the formation of new adducts resulting from the combination of polystearylmethacrylate (PSMA) and trimethylaluminum (TMA), PM6 calculations were performed by obtaining coherent results following experimental data.

For the reasons presented above, we studied the enhancement of the catalytic system under optimal conditions. The polymer-stabilized co-catalysts were investigated in slurry polymerization of ethylene, leading to polyethylene (PE) with higher bulk densities, associated with a change in particle morphology, compared with the polyethylene obtained using a conventional methylaluminumoxane co-catalyst. These results embody a substantial enhancement upon prior efforts [17] to optimize production costs, by achieving superior morphology and reduction of inorganic residues in the synthesized polyolefins.

EXPERIMENTAL

Reagents

TMA 2M in toluene (Sigma-Aldrich), MMAO-12 at 7% Al m/m in toluene (Sigma-Aldrich), and PSMA

synthesized via RAFT of 8,900 g/mol, $\bar{D} = 1.11$ (supplied by Friedrich Schiller University Jena) were used. Toluene and anhydrous hexane (Sigma-Aldrich) were used as solvents. Anhydrous inhibitor-free THF (99.9%, Sigma-Aldrich) was used without previous distillation. All reagents were stored under a dry nitrogen atmosphere.

Instrumentation

Nuclear magnetic resonance (NMR) spectra were acquired in a *Bruker Avance III HD* 400 MHz NMR spectrometer equipped with a 5 mm BBI multi-nuclear probe. Sample preparation for NMR was performed under nitrogen atmosphere in 5 mm tubes with an evacuation valve, using 0.5 mL of the analyte and 0.1 mL of C₆D₆. The acquisition was performed at 27°C. FT-IR analysis was carried out on a Thermo-Scientific Nicolet 6700 FTIR spectrophotometer and samples were placed in a liquid cell and prepared under nitrogen atmosphere in the glove box by injecting 0.3 mL of analyte (at the concentration resulting after performing the respective reaction) into the cell.

Dynamic light scattering (DLS) measurements were performed in a Microtrac Nanotrak Wave II spectrophotometer using a stainless-steel cell with a sapphire window containing 1 mL of analyte at a concentration of 0.1 g/mL prepared under nitrogen atmosphere.

Differential scanning calorimetry (DSC) analyses of the polymers obtained were carried out by employing a TA Instruments® DSC 2500 Discovery Series differential scanning calorimeter, and using 0.0093 g of sample in N₂/O₂ atmosphere with a heating ramp of 10°C min⁻¹.

The GPC/SEC samples were prepared by dissolving the polymer samples in trichlorobenzene at a concentration of 1.57 g mL⁻¹ and an injection volume of 200 μL on an Agilent Technologies® PL-GPC 220 instrument equipped with a set of cross-linked polystyrene linear columns (PLgel 10 μM). The total run time was 65 min, at 140°C. Universal calibration was applied over a 1.95 - 3.25 K MW range with PSty standards and adjusted for high-temperature studies.

The bulk density of the raw materials was measured using ASTM D1895B standard procedure.

MMAO-12 composition determination

MMAO-12 is defined as a co-polymer that has one

block of n-octylaluminumoxane and one block of methylaluminumoxane. To determine the size of each block as well as the amount of TMA, a $^1\text{H-NMR}$ determination was performed by applying the method described by Imhoff et al [18].

Treatment of PSMA with TMA

To a dry 10 mL vial, 0.6667 g (7.49×10^{-2} mmol) of PSMA was added and dissolved in 5 mL of hexane. After degassing the solution by ultrasonication, 1 mL (2 mmol) of 2 M TMA in toluene was added, the resultant mixture had an Al/C=O ratio of 1. The sample was left at room temperature for 4 h. After this time, the respective characterization by $^1\text{H-NMR}$, $^1\text{H-DOSY}$, and FT-IR of the sample was carried out.

Reactions between PSMA, TMA, and MMAO-12

0.06 g ($8,900 \text{ g mol}^{-1}$) of PSMA (6.74×10^{-3} g or 0.177 mmol in ester groups) were added to a vial followed by 5 mL of hexane. After dissolving the PSMA, the solution was degassed by ultrasound. 1 mL of TMA 2 M (2 mmol) was added followed by 2 mL of MMAO-12 2.4 M (4.8 mmol) corresponding to an Al/O ratio of 40 (total aluminum to carbonyl oxygen). The resulting solution remained at room temperature for 4 h and was subsequently characterized by $^1\text{H-NMR}$, $^1\text{H-DOSY}$, and DLS.

Ethylene polymerizations trials

A stainless-steel batch reactor with a 600 mL glass vessel was previously dried at 130°C for 12 h. The reactor and vessel were dried again for 1 h under vacuum at 80°C . The vessel was then loaded with 60 mL of dry hexane followed by three argon/vacuum purges. To the mixture of the PSMA/TMA/MMAO-12 co-catalyst, 0.003 g (7.41×10^{-3} mmol) of bis(n-butylcyclopentidine) zirconium dichloride ($(\text{n-BuCp})_2\text{ZrCl}_2$), dissolved in 1 mL of toluene, was added inside a dry box (under N_2 atmosphere). The final mixture was injected into the reactor vessel using a syringe and the stirrer was adjusted to 800 rpm. Finally, the ethylene consumption recording system was turned on and the ethylene valve was opened. The pressure was set at 42 psi followed by data recording using an acquisition routine in Labview®. After one hour, the data logging and stirring were stopped, the ethylene valve was

shuttled off and the reactor was allowed to cool to room temperature at which time the remaining ethylene pressure was released. After this, 10 mL of acidified methanol was added to quench the reaction. Three methanol washes followed by one hexane wash were performed. The filtered product was dried for 24 h at 60°C and then weighted.

Computational details

One conformational unit of the PSMA including end groups (PSMA1u) was modeled and optimized (as a global calculation) using the PM6 method implemented in Wavefunction Spartan 14®. Once optimized, a TMA molecule was attached via the C=O group and this new structure (PSMA1u-TMA) and its thermodynamics were calculated using PM6, verifying a true minimum as no imaginary frequencies were obtained in the corresponding vibrational spectrum.

RESULTS AND DISCUSSION

Total TMA present in MMAO-12

The incorporation of n-octyl groups into the methylaluminumoxane (MAO) is carried out to make it more soluble in non-polar media. This co-polymer usually has several structures, both linear and box-like [19] so, the product is sold as a 7% w/w aluminum solution in toluene with varying amounts of trimethylaluminum (TMA). Moreover, this amount of TMA is known to directly influence the activating capacity of the mixture when reacting with group 4 metallocenes for the synthesis of polyethylenes [20]. The typical $^1\text{H-NMR}$ spectrum of MMAO-12 is depicted in Figure 1a. Figure 1b shows the result of the experiment carried out with the addition of anhydrous THF for the quantitative determination of its chemical composition.

Figure 1b depicts how the addition of THF produces a Lewis adduct, identified by the appearance of two new signals at low frequency (-0.56 ppm, -0.62 ppm). The one at the lower frequency corresponds to free TMA while the one to its right corresponds to the activating species or Me_2Al^+ ; the broad signal corresponds to methylaluminumoxane. After a careful integration of the region between 0 and -1 ppm using signal deconvolution, the following results were obtained

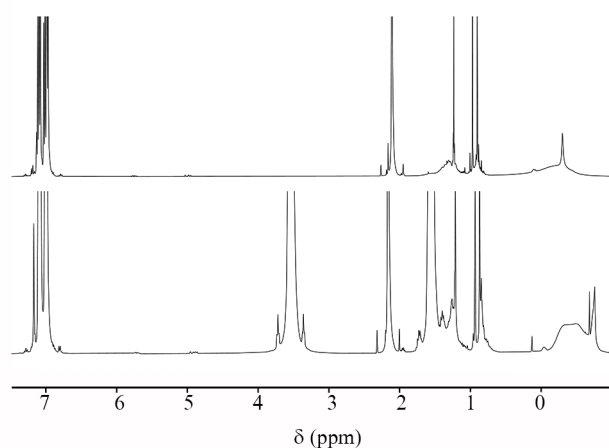


Figure 1. $^1\text{H-NMR}$ (C_6D_6 , 400 MHz) for MMAO-12 solution (a), and MMAO-12 solution + 10 eq. of dry THF (b).

regarding the composition of MMAO-12: methylaluminumoxane 94 %mol; n-octylaluminumoxane 6 %mol; Me_2Al^+ 2.62 %mol; TMA (free) 4.74 %mol; TMA (total) 7.36 %mol. This analysis indicates that only 2.62 %mol of the total TMA can be ionized into activating species when using oxygenated donors.

Characterization and hydrodynamic diameter of PSMA

The typical $^1\text{H-NMR}$ spectrum of PSMA ($8,900 \text{ g mol}^{-1}$) is shown in Figure 2. The signals of the main chain can be identified whereas the end groups cannot since these relative intensities are very diluted concerning the others. An effect of benzene- d_6 (interaction between π -bonds) is also observed by the splitting of the signal centered in 4.13 ppm, so changes in this region indicate different chemical behaviors by the carbonyl group in the next experiments presented in

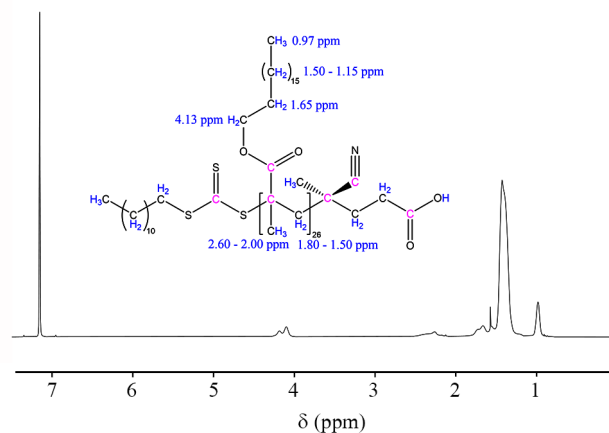


Figure 2. $^1\text{H-NMR}$ (C_6D_6 , 400 MHz) for the RAFT-synthesized PSMA.

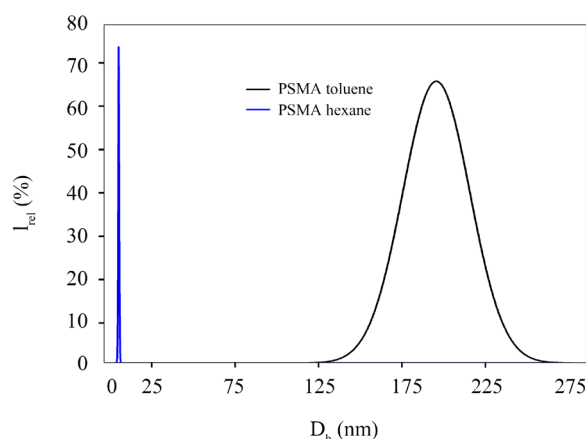


Figure 3. Hydrodynamic diameter for PSMA in hexane (blue), and toluene (black) measured by DLS.

this work.

After properly identifying the structure of PSMA, its behavior in two different solvents was determined by DLS. Two different solutions of PSMA at 0.1 g mL^{-1} were analyzed by DLS and by obtaining the following D_h 's. Figure 3 depicts a broad population of PSMA with a $D_h = 202.5 \text{ nm}$ in toluene whereas a smaller average size and distribution is observed in hexane $D_h = 4.75 \text{ nm}$. These two solvents have low polarity, but toluene has π -character, the result indicates a trend regarding the nature of the solvent. If the π -character of solvent is decreased, the hydrodynamic diameter of the polymer decreases as well. Since the goal here is to construct robust co-catalyst particles based on PSMA-MMAO, the solvent chosen for testing interactions and ethylene polymerization media was hexane.

Interactions between PSMA and TMA

To comprehend the nature of the interactions that occur between PSMA and TMA, several spectroscopic studies were carried out. Figure 4 compares free PSMA (Figure 4a), free TMA (Figure 4b), and the mixture 1:1 ($\text{C}=\text{O}:\text{Al}$) of PSMA and TMA at 300 K (Figure 4c). The most relevant feature in the mixture is the convergence of the (previously seen) split signal for the $-\text{CH}_2-\text{O}-$ groups into one which has also shifted from 4.13 ppm to 4.22 ppm. Also, a shift in the CH_3-Al is observed from -0.39 ppm to -0.58 ppm . This un-splitting means that somehow the initial conformation of the ester chains has changed. In addition, the shifting of these two signals also describes an interaction between $\text{C}=\text{O}$ and aluminum (III).

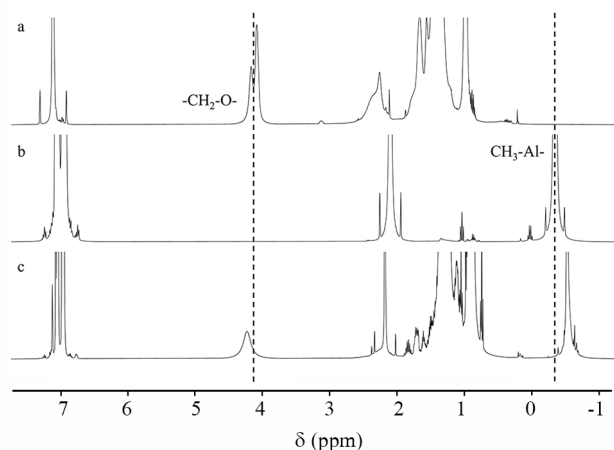


Figure 4. $^1\text{H-NMR}$ (C6D6, 400 MHz) for the PSMA (a), TMA (b), and the mixture of PSMA+TMA 1:1 C=O/Al (c).

However, since the CH_3 - signal for toluene also shifted from 2.07 ppm to 2.16 ppm, a $^1\text{H-DOSY}$ was performed to prove any interaction between the carbonyl oxygen and aluminum (III) and not shifting by the polarity of the mixture. Figure 5 shows a typical DOSY spectrum (upper section) for this kind of mixture and as can be seen the diffusion rate for the $-\text{CH}_2\text{-O-}$ and $\text{CH}_3\text{-Al-}$ signals is the same. This indicates that the two species diffuse as a whole and confirm the formation of a new adduct.

The FT-IR analysis for the mixture also shows a hypsochromic shift for the C=O band from 1737 cm^{-1} to 1744 cm^{-1} , proving the coordination of the oxygen to aluminum (III) in non-polar media as depicted in Figure 6 [21].

Computational calculations using the PM6 semi-empirical method also show favorable thermodynam-

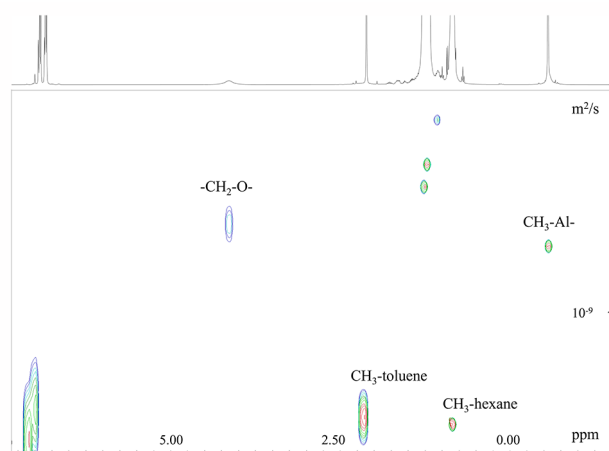


Figure 5. $^1\text{H-DOSY}$ spectrum for the mixture of PSMA+TMA 1:1 C=O/Al.

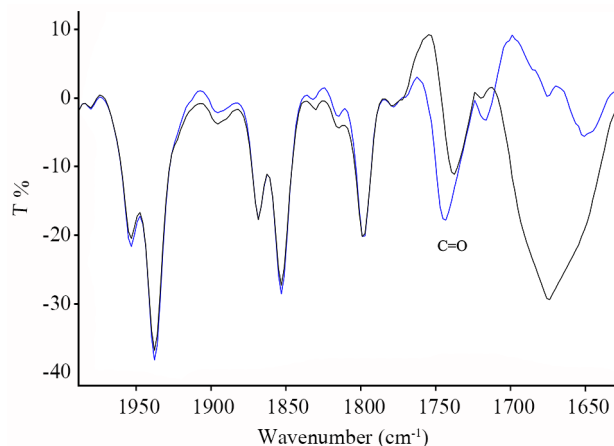


Figure 6. FTIR spectrum for the of PSMA (black), and PSMA+TMA 1:1 C=O/Al in the range of ester carbonyls.

ics regarding the formation of a coordination adduct. To simplify the model, one repeating unit of PSMA (PSMA1u) interacts with a single molecule of TMA (Figure 7) resulting in free energy of $\Delta G_f = -0.40\text{ Kcal mol}^{-1}$ at 298.15 K, showing a slightly spontaneous reaction. Since the PSMA has 26 repeating units, the coordination by the carboxyl oxygen occurs 26 times, thus lower free energy can be expected for the total amount of these interactions. The increase of temperature has a positive thermodynamic effect on the coordination because of the decrease of the $T\Delta S$. This result agrees with the spectroscopic data.

The co-catalyst mixture PSMA/TMA/MMAO-12

After mixing PSMA and MMAO-12 with an equal ratio of $\text{C=O}:\text{Al}$, different behavior is observed. $^1\text{H-NMR}$ in Figure 8 shows a consumption of the TMA present in the MMAO-12 solution. A CH_4 is present near 0.18 ppm which is consistent with a reaction with the $-\text{COOH}$ end group of the PSMA as previously reported by Slaughter et al [22].

Since TMA is responsible for the activation of the catalyst, some changes need to be applied to avoid this undesirable reaction. The initial guess is to add more

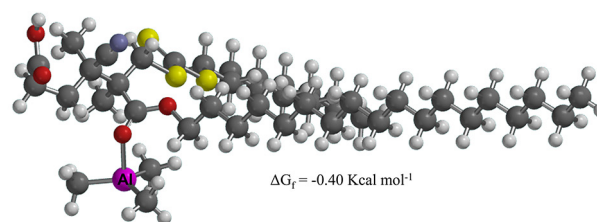


Figure 7. PM6-optimized structure for PSMA1u + TMA.

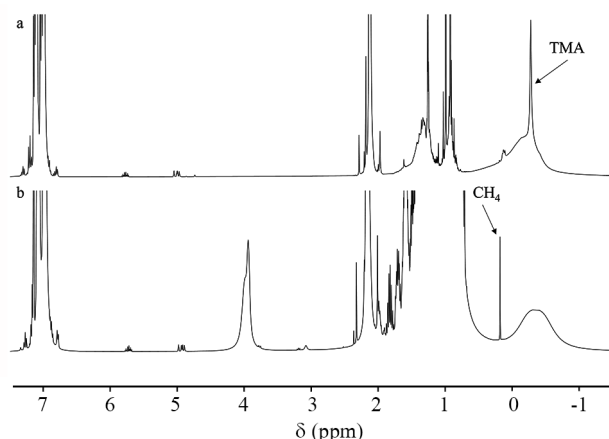


Figure 8. $^1\text{H-NMR}$ (C_6D_6 , 400 MHz) of MMAO-12 (a), and PSMA + MMAO-12 1:1 C=O/Al (b).

TMA to guarantee the composition of the MMAO-12, the second is to reduce the amount of PSMA to 10 %mol for the initial amount used. In this new mixture, it is possible to take advantage of the bridging capacity of the TMA via methyl groups [11], and the coordination of the PSMA to TMA via C=O groups as depicted in Figure 9.

The new co-catalyst mixture based on PSMA/TMA/MMAO-12 has a C=O:TMA:MMAO-12 ratio of 1:11.3:27, respectively. The reason for using 10 %mol of PSMA concerning the initial condition is related to the TMA amounts present in MMAO-12 solutions which were determined to be about 7.36 %mol. The additional TMA compensates for any undesired reaction as well as works as an in-situ scavenger in further polymerization reactions.

The $^1\text{H-NMR}$ for this mixture is shown in Figure 10. As can be seen, there is less methane evolution as witnessed by the signal in 0.18 ppm. Also, the un-splitting of the signal in 4.42 ppm corresponding to the $-\text{CH}_2-\text{O}-$ group is evidenced, confirming coordination by the C=O of PSMA. This signal is also broadened

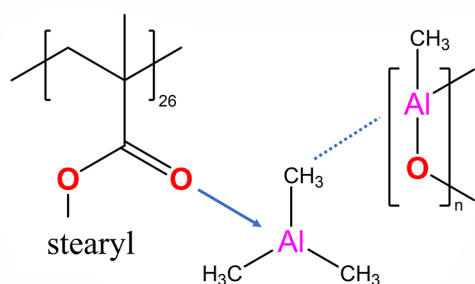


Figure 9. Interactions between PSMA, TMA, and MMAO-12.

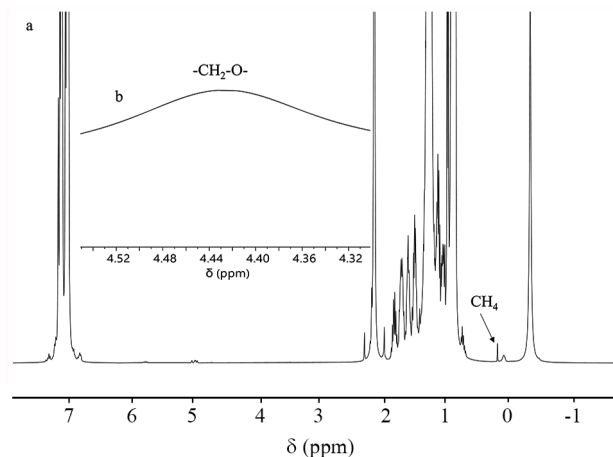


Figure 10. $^1\text{H-NMR}$ (C_6D_6 , 400 MHz) for the mixture of PSMA/TMA/MMAO-12 (a), and a magnification of the $-\text{CH}_2-\text{O}-$ region (b).

due to the reduction in the concentration of the PSMA.

Since the objective is to form a robust co-catalyst particle to directly influence the polyethylene growth, a DLS study of this mixture at 25°C in the solvent mixture resulting from the reaction crude (62.5% v/v hexane, 37.5% v/v toluene) was carried out, finding a D_h of 27.05 nm as seen in Figure 11, confirming the heterogenization of the system at nano-scale.

Ethylene polymerization trials

Once the co-catalyst system was studied, a few ethylene polymerization trials were performed. In Table 1 a resume of each experiment is presented. The differences in terms of BD are evident for the co-catalyst based on PSMA/TMA/MMAO-12 when compared to a blank reaction and when using a different neutral donor (OMTS, 1,1,1,3,3,5,5,5-octamethyltrisiloxane). Best

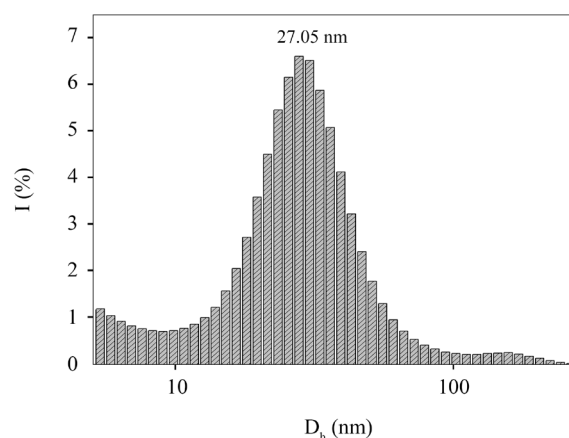


Figure 11. Hydrodynamic diameter for the mixture PSMA/TMA/MMAO-12 measured by DLS.

Table 1. Results obtained for the polymerization of ethylene using co-catalysts based on PSMA/TMA/MMAO-12.

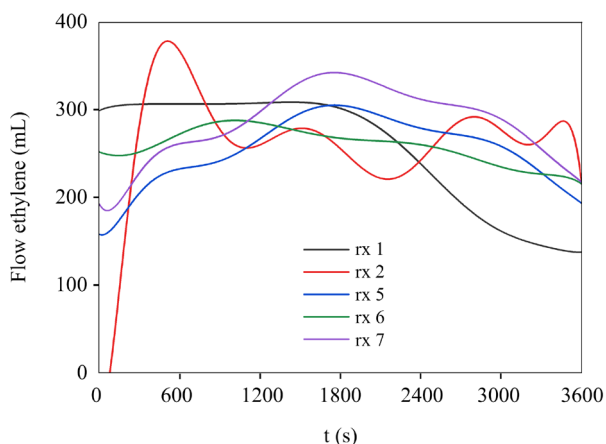
Reaction	Co-catalyst	Catalyst	Al/Zr			Al/O	A (Kg PE molZr ⁻¹ h ⁻¹)	BD (g cm ⁻³)
			TMA	MMAO-12	Total			
0	TMA	(<i>n</i> -BuCp) ₂ ZrCl ₂	800	0	800	0	0	0
1	TMA/MMAO-12	(<i>n</i> -BuCp) ₂ ZrCl ₂	249	584	833	0	1885	0.26
2	OMTS/MMAO-12	(<i>n</i> -BuCp) ₂ ZrCl ₂	0	800	800	76	2667	0.22
3	PSMA/TMA/MMAO-12	(<i>n</i> -BuCp) ₂ ZrCl ₂	830	0	830	1	94	0
4	PSMA/TMA/MMAO-12	(<i>n</i> -BuCp) ₂ ZrCl ₂	75	175	250	40	0	0
5	PSMA/TMA/MMAO-12	(<i>n</i> -BuCp) ₂ ZrCl ₂	253	585	838	40	1543	0.33
6	PSMA/TMA/MMAO-12	(<i>n</i> -BuCp) ₂ ZrCl ₂	220	583	807	40	1311	0.40
7	PSMA/TMA/MMAO-12	(<i>n</i> -BuCp) ₂ ZrCl ₂	247	583	830	40	1847	0.43

bulk densities were obtained in reaction 7.

From Table 1, the effect of PSMA over BD is evident. Though, there is a penalty in terms of the activity when compared to reaction 2 which uses OMTS as the donor. By this means, an inverse relationship between BD and activity can be established.

The ethylene consumption profile also shows differences (Figure 12). The typical reaction using MMAO-12 (reaction 1) drops in ethylene consumption at 1800 s whereas the reaction with neutral donors continues consuming even at 3300 s with a similar rate. The control experiment using OMTS as a donor exhibits an oscillating profile at different stages of the reaction, in agreement with a highly reactive system. These profiles also indicate that the residence times (RTD) for all modified co-catalyst results increased with respect to the blank reaction (rx 1). This effect can be extended to continuous processes by reducing the amount of catalytic system used and thus decreasing the feeding frequency.

In Table 2, the properties of the synthesized materials are shown. In general, the \bar{D} is comparable for all the materials except for the blank which has a narrower

**Figure 12.** Ethylene consumption profiles on polymerization reactions using OMTS and PSMA/TMA/MMAO-12.**Table 2.** Molar mass for the synthesized polyethylenes.

Reaction	M_n (g/mol)	M_w (g/mol)	M_z (g/mol)	M_v (g/mol)	\bar{D}	T_m (°C)
1	13,455	26,665	43,946	41,602	1.98	131.5
2	27,486	96,658	231,214	485,354	3.51	132.9
5	7,355	24,296	107,252	88,431	3.30	132.5
6	6,229	17,282	58,670	50,288	2.77	130.3
7	13,947	43,538	266,858	204,776	3.12	131.4

\bar{D} but, regarding molar mass, huge differences can be appreciated. Using OMTS as a donor leads to a more reactive catalytic system, so higher molar masses are observed. On the other hand, when using PSMA, a stabilizing effect can be observed as the slowly growing of the molar mass. Since higher BD's are useful to avoid or decrease fouling in reactors, a slow-growing molar mass is preferred instead of a highly reactive system. It is important to remark that the polyethylene synthesized by this method led to monomodal HDPE unlike the CX or Hostalen processes [23, 24]. Also, commercial processes on slurry phase based on magnesium dichloride/alquialuminum as the catalytic system had shown typical average BD's between 0.26 and 0.39 g cm⁻³ [25].

CONCLUSIONS

The effect of a neutral polymeric donor over BD of polyethylene was studied by obtaining up to 0.43 g cm⁻³ in typical polymerization reactions. The nature of the interactions that happen between the carbonyls and aluminum (III) in low polarity media was studied using spectroscopic data from ¹H-NMR, ¹H-DOSY, DLS, and FT-IR, showing coordination by the carbonylic oxygen to the aluminum center of the TMA which is favorable ($\Delta G_f = -0.40$ kcal mol⁻¹). Also,

the formation of this adduct introduces a stabilizing effect over the polymerization of ethylene, allowing the obtention of HDPE with a high BD (0.43 g cm^{-3}) due to a slowly growing of the molar mass. Other neutral donors like OMTS do not have an advantageous effect on BD (since it is a small molecule) but into activity. Thus, the use of PSMA as the oxygen-neutral donor has an inverse relationship in terms of activity and BD. A small molecule such as OMTS allows higher activities at the expense of a poor BD whereas a polymeric additive like PSMA introduces higher BDs but not so-high activities. This work unlocks a new approach for the use of polymeric additives to achieve higher BDs which can prevent fouling, instead of the use of traditional supported catalyst systems or the most used slurry phase processes commercially available based on magnesium dichloride/alkylaluminum. Also, the increased residence time concerning blank reactions can be useful when using continuous processes instead of batch polymerizations.

ACKNOWLEDGEMENTS

The authors thank Dr. Carlos Guerrero-Sánchez and the Friederich-Schiller University of Jena for facilitating the RAFT-synthesized polymer additive (PSMA).

CONFLICTS OF INTEREST

The authors declare that they have no conflicts of interest.

REFERENCES

1. Kaminsky W (1994) Zirconocene catalysts for olefin polymerization. *Catal Today* 20: 257-270
2. Kaminsky W, Duch A (1996) New developments in olefin polymerization with metallocene catalysts. *Catalysts in petroleum refining and petrochemical industries*, 1st ed., Elsevier, 91-98
3. Kaminsky W (1998) Highly active metallocene catalysts for olefin polymerization. *J Chem Soc Dalton* 9: 1413-1418
4. Lee BY, Chung YK, Lee SW (1999) Synthesis of bis(1,2,3-substituted cyclopentadienyl) zirconium dichloride derivatives and their use in ethylene polymerization. *J Organomet Chem* 587: 181-190
5. Lee KS, Yim JH, Ihm SK (2000) Characteristics of zirconocene catalysts supported on Al-MCM-41 for ethylene polymerization. *J Mol Catal A-Chem* 159: 301-308
6. Pothirat T, Jongsomjit B, Praserttham P (2008) A comparative study of SiO_2 - and ZrO_2 -supported zirconocene/MAO catalysts on ethylene/1-olefin copolymerization. *Catal Commun* 9: 1426-1431
7. Laine A, Linnolahti M, Pakkanen TA (2012) Alkylation and activation of metallocene polymerization catalysts by reactions with trimethylaluminum: A computational study. *J Organomet Chem* 716: 79-85
8. Zijlstra HS, Joshi A, Linnolahti M, Collins S, Mcindoe JS (2018) Modifying methylalumoxane via alkyl exchange. *Dalton Trans* 47: 17291-17298
9. Zijlstra HS, Joshi A, Linnolahti M, Collins S, Mcindoe JS (2019) Interaction of neutral donors with methylaluminoxane. *Eur J Inorg Chem* 2019: 2346-2355
10. Joshi A, Collins S, Linnolahti M, Zijlstra HS, Liles E, Mcindoe JS (2021) Spectroscopic studies of synthetic methylaluminoxane: Structure of methylaluminoxane activators. *Chem-Eur J*
11. Linnolahti M, Collins S (2017) Formation, structure, and composition of methylaluminoxane. *Chem Phys Chem* 18: 3369-3374
12. Belelli PG, Castellani NJ (2003) DFT studies of Zirconocene/MAO interaction. *J Mol Catal A-Chem* 192: 9-24
13. Tymińska N, Zurek E (2015) DFT-D investigation of active and dormant methylaluminoxane (MAO) species grafted onto a magnesium dichloride cluster: A model study of supported mao. *ACS Catal* 5: 6989-6998
14. Ustynyuk LY, Bulychev BM (2015) Activation effect of metal chlorides in post-metallocene catalytic systems for ethylene polymerization: A DFT study. *J Organomet Chem* 793: 160-170

15. Ferreira ML, Damiani ED, Juan A (1998) Semiempirical study of metallocenes adsorption on β - MgCl_2 . *Comput Mater Sci* 9: 357-366
16. Stewart JJ (2009) Application of the PM6 method to modeling proteins. *J Molecul Model* 15: 765-805
17. Estrada-Ramirez AN, Ventura-Hunter C, Vitz J, Díaz-Barriga E, Peralta-Rodriguez R, Schubert US, Guerrero-Sánchez C, Pérez-Camacho O (2019) Poly(n-alkyl methacrylate)s as metallocene catalyst supports in nonpolar media. *Macromol Chem Phys* 220: 1900259
18. Imhoff DW, Simeral LS, Blevins DR, Beard WR (1999) Determination of trimethylaluminum and characterization of methylaluminumoxanes using proton NMR. In: *Olefin Polymerization. ACS symposium series 749*: 177-191
19. Beelli PG, Castellani NJ (2006) Counterion and additive effects on ethylene coordination and insertion in metallocene catalyst. *J Mol Catal A-Chem* 253: 52-61
20. Blaakmeer ESM, van Eck ERH, Kentgens APM (2018) The coordinative state of aluminium alkyls in Ziegler-Natta catalysts. *Phys Chem Chem Phys* 20: 7974-7988
21. Nakamoto K (2009) Infrared and Raman spectra of inorganic and coordination compounds. Part A: Theory and applications in inorganic chemistry, 6th ed., Wiley, 192-213
22. Slaughter J, Peel AJ, Wheatley AE (2017) Reactions of trimethylaluminium: Modelling the chemical degradation of synthetic lubricants. *Chemistry* 23: 167-175
23. Knuuttila H, Lehtinen A, Nummila-Pakarinen A (2004) Advanced Polyethylene Technologies-Controlled Material Properties. *Adv Polym Sci* 169, 13-28
24. Malpass DB (2010) Introduction to Industrial Polyethylene Properties, Catalysts, and Processes, Wiley-VCH, Ch. 1: 52-55; 91-93
25. Wang D, Yang G, Guo F, Wang J, Jiang Y (2018) Progress in technology and catalysts for continuous stirred tank reactor type slurry phase polyethylene processes. *Petrol Chem* 58: 264-273